Radiative electron capture and the photoelectric effect at high energies

A. Ichihara and T. Shirai
Japan Atomic Energy Research Institute, Tokai-mura, Ibaraki 319-11, Japan

Jörg Eichler*
Bereich Theoretische Physik, Hahn-Meitner-Institut Berlin, 14109 Berlin, Germany
and Fachbereich Physik, Freie Universität Berlin, 14195 Berlin, Germany
(Received 21 June 1996)

In high-energy atomic collisions between bare high-Z projectiles and low-Z target atoms, an electron may be captured radiatively into the projectile [radiative electron capture (REC)]. The photon angular distributions can be very well represented by radiative recombination (RR) of the projectile with free electrons. This process is the inverse of the photoelectric effect. In this paper, we present exact differential RR cross sections for Au^{79+} and U^{92+} at projectile energies of 0.2, 0.5, 1, 2, 5, and 10 GeV/u. We also show the differential cross sections for the photoelectric effect at x-ray energies corresponding to the former projectile energies. It is seen that because of the dramatic forward-peaking of the cross sections at high energies, measurements of REC from low-Z targets are the most practical way to study the photoelectric effect. In one particular example, 10.8 GeV/u Au^{79+} on Au targets, we show that the RR cross section multiplied with the number of target electrons is very close to the REC cross section calculated within the impulse approximation. [S1050-2947(96)08511-3]

PACS number(s): 34.70.+e, 32.80.Fb

I. INTRODUCTION

With present-day accelerators, it is possible to produce relativistic beams of bare or almost bare high-Z ions [1]. If one of these ions collides with a low-Z target atom, it may capture an electron, with a simultaneously emitted photon carrying away the excess energy and momentum. Since the loosely bound target electrons can be considered as quasifree, radiative electron capture (REC) is almost identical to radiative recombination (RR), which is the inverse of the photoelectric effect [2,3]. Indeed, for systems such as Au^{79+} or U^{92+} on N_2 targets, this is an excellent approximation. From the experimental point of view, REC is the dominant charge changing processes.

In an earlier publication [1,2], motivated by the feasibility of experiments, we had formulated the exact theory of REC for relativistic collisions. Since then, the theoretical results have been confirmed by a large number of experimental measurements by Stöhlker and co-workers [4–8], including capture into the L shell [5] and into the M shell [8]. It turned out that for high-Z high-energy projectiles, the angle-differential cross section deviates significantly from the $\sin^2\theta$ distribution originally found for 197 MeV/u Xe^{54+} projectiles on Be atoms [9]. A systematic theoretical study of RR cross sections by Eichler *et al.* [3] derives the basic qualitative features in an analytic form from angular-momentum conservation and a simple approximate treatment. Furthermore, exact differential K-, L-, and M-REC cross sections for a series of projectile charges and energies have been presented, demonstrating the limitations of a $\sin^2\theta$ distribution, which is often assumed in evaluating experimental total cross sections. It is concluded that in REC angular distributions, the electron spin manifests itself in a particularly clear-cut way.

In the present study, we improve the numerical methods in order to carry the systematics to much higher energy than considered so far. We also find it instructive to compare a set of differential RR cross sections with the corresponding cross sections for the photoelectric effect. In Sec. II, we describe the basic assumptions of our calculations. In Sec. III, we first give a systematics of differential cross sections for radiative recombination (equivalent to REC) and also the corresponding cross sections for the photoelectric effect. Furthermore, in a specific example, we compare REC cross sections calculated from Hartree-Fock momentum distributions in the target with RR cross sections. Finally, in Sec. IV, we summarize our conclusions.

II. CALCULATIONS

In our formulation [2], we start with an exact treatment of the photoelectric effect assuming a Coulomb-Dirac wave function $\psi_{j_b,\mu_b}(\mathbf{r})$ for an arbitrary initial bound state and, correspondingly, an exact Coulomb-Dirac continuum wave function $\psi_{\mathbf{p},m_s}(\mathbf{r})$, given by the usual partial wave expansion. The transition matrix element is

$$M_{\mathbf{p},b}(m_s,\lambda,\mu_b)=\int \psi^{\dagger}_{\mathbf{p},m_s}(\mathbf{r})\vec{\alpha}\cdot\hat{\mathbf{u}}_{\lambda}e^{i\mathbf{k}\cdot\mathbf{r}}\psi_{j_b,\mu_b}(\mathbf{r})d^3r, \tag{1}$$

where $\vec{\alpha}$ is the Dirac alpha matrix, $\mathbf{k}$, with $k=\omega/c$, is the wave vector, and $\hat{\mathbf{u}}_{\lambda}$ is the unit vector of photon polarization. In the photon wave function, the full retardation, that is, all multipoles, are included. Within the continuum wave function $\psi_{\mathbf{p},m_s}(\mathbf{r})$, the partial-wave expansion is carried to a maximum Dirac quantum number $|\kappa_{\max}|$ as required by convergence. The radial integration is performed numerically.

*Electronic address: eichler@hmi.de

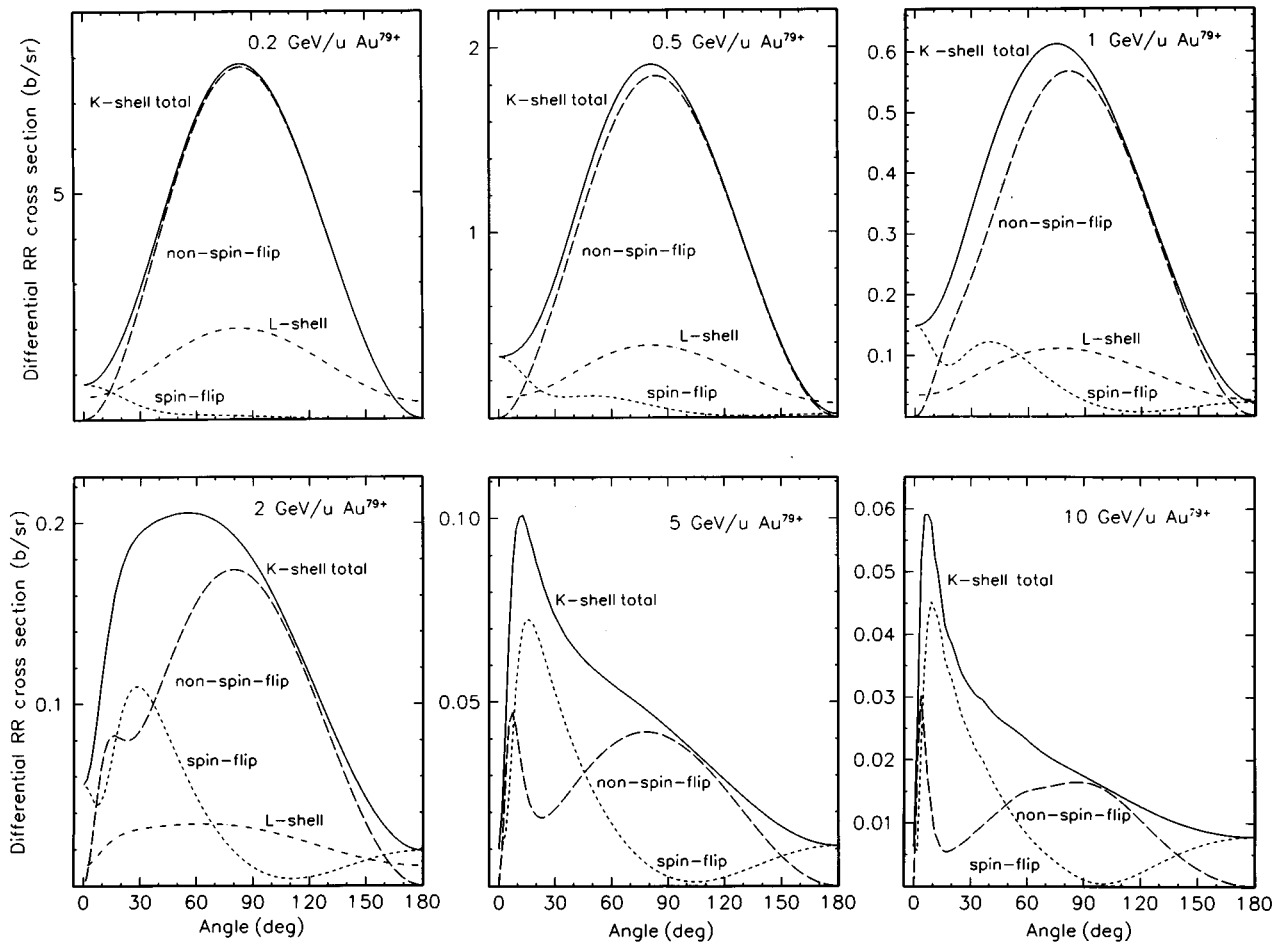

FIG. 1. Exact angle-differential cross sections for radiative recombination of free electrons with the K shell of Au^{79+} projectiles with energies from 0.2 to 10.0 GeV/u. The spin-flip and non-spin-flip contributions are shown separately. For energies up to 2.0 GeV/u, the summed cross section for capture into the L shell is also shown.

The probabilities obtained from Eq. (1) are summed over the unmeasured quantum numbers m_s, λ, and μ_b and are integrated over the impact-parameter plane.

In order to derive RR cross sections in the projectile frame from the calculated photoelectric cross sections, we first apply the principle of detailed balance to describe the inverse reaction and subsequently perform a Lorentz transformation from the projectile frame to the laboratory frame. This transformation is achieved by substituting

$$\cos\theta = \frac{\cos\theta_{\rm lab} - \beta}{1 - \beta\cos\theta_{\rm lab}} \tag{2}$$

and

$$\frac{d\sigma(\theta_{\rm lab})}{d\Omega_{\rm lab}} = \frac{1}{\gamma^2(1-\beta\cos\theta_{\rm lab})^2}\frac{d\sigma(\theta)}{d\Omega}, \tag{3}$$

where $\beta = v/c$ and $\gamma = 1/\sqrt{1-\beta^2}$.

Starting from the general computer code [2], but modifying it so as to include higher electronic partial waves and higher photon multipoles, we perform calculations of the differential cross sections for the photoelectric effect and radiative recombination. In order to check our calculations, we compare our differential cross sections for the photoelectric effect in the K shell with the results of Alling and Johnson [10]. Even for the highest photon energy $\hbar\omega = 1.332$ MeV, we obtain very good agreement, our results being probably more accurate since they include higher partial waves.

The number of partial waves required for the convergence of the calculation depends on the energy E_P of the projectile. For the K shell and $E_P \leqslant$ 1.0 GeV/u we use $|\kappa_{\rm max}| = 20$, for $E_P =$ 2.0 GeV/u we use $|\kappa_{\rm max}| = 30$, for $E_P =$ 5.0 GeV/u we use $|\kappa_{\rm max}| = 60$, and for $E_P =$ 10.0 GeV/u we use $|\kappa_{\rm max}| = 80$. For radiative recombination with the L shell, one needs higher partial waves. Already at $E_P =$ 2.0 GeV/u we need $|\kappa_{\rm max}| = 50$, and for $E_P = 5.0$ GeV/u we were no longer able to achieve convergence, even with $|\kappa_{\rm max}| = 80$.

In some calculations, we take into account the momentum distribution of the target electrons provided by a nonrelativistic Roothaan-Hartree-Fock approach using the Slater double-ζ functions [11].

III. RESULTS AND DISCUSSION

A. Differential RR and photoelectric cross sections

In Figs. 1 and 3, we present the results of systematic calculations of differential cross sections for radiative recombination (which are almost identical to those for REC) assuming bare Au^{79+} and U^{92+} projectiles which both play a role in present experiments. With the projectile energies E_P

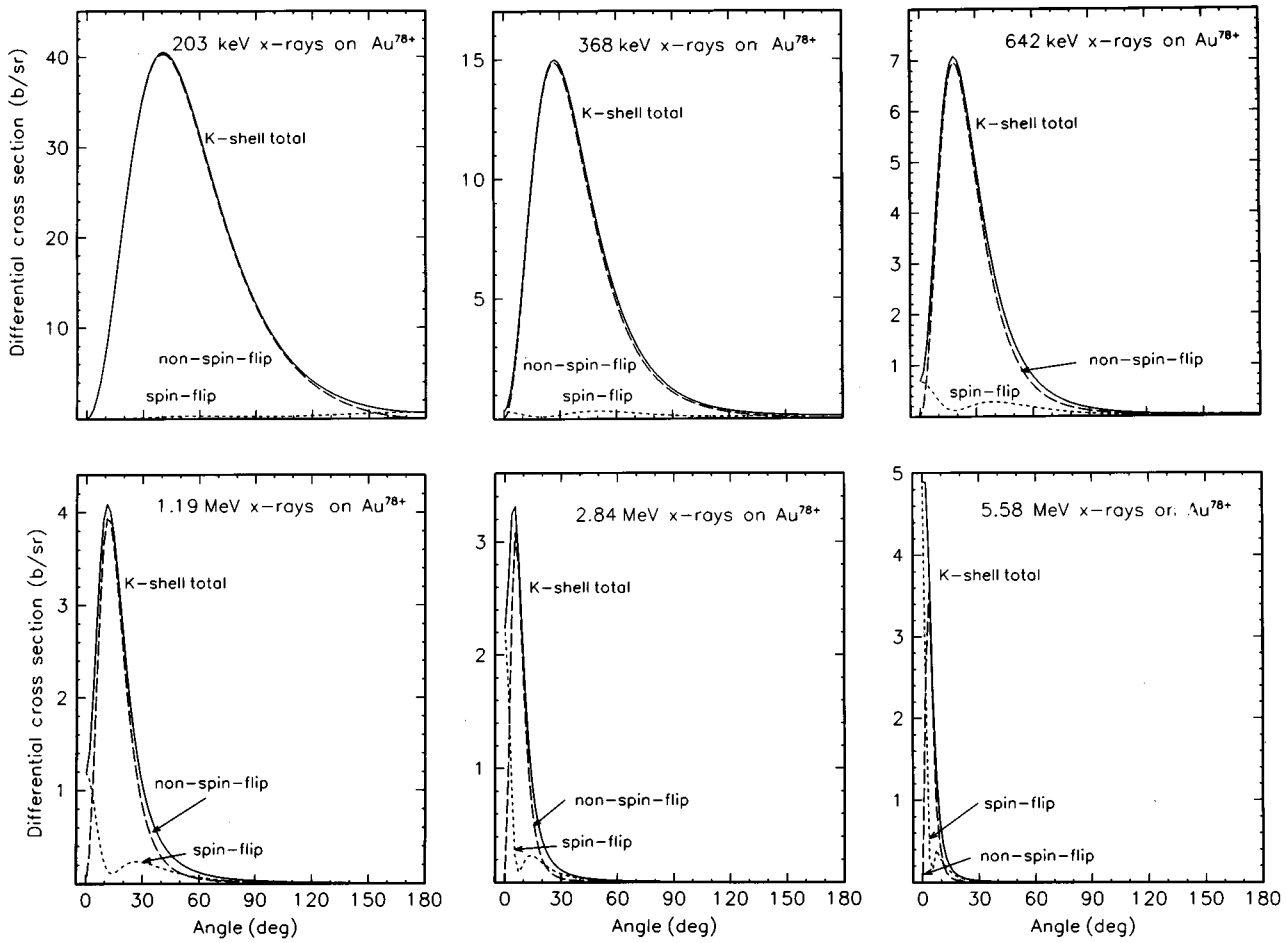

FIG. 2. Exact angle-differential cross sections for photoionization from the K shell of hydrogenlike Au^{78+} ions. The x-ray energies given correspond to the projectile energies used in Fig. 1.

of 0.2, 0.5, 1.0, 2.0, 5.0, and 10.0 GeV/u, we extend earlier calculations [3] to much higher energies. As an additional feature, we provide in Figs. 2 and 4, associated with each set of RR cross sections, the differential cross sections for the photoelectric effect at the x-ray energies corresponding to the projectile energies given above. In other words, the capture into the projectile of free electrons traveling with the target speed towards the projectile, leads to the *emission* of x rays with a definite energy E_γ. The corresponding photoeffect consists of the *absorption* of x rays with energy E_γ and the emission of electrons with the relative target-projectile velocity. Similar to [10], the photoelectric cross sections are not divided by the multiplicity $(2j+1)$ of the initial states.

As a remarkable feature, we observe that up to an energy of 1.0 GeV/u, the RR cross sections still roughly follow a $\sin^2\theta$ distribution, the deviations being mainly caused by the spin-flip contribution as discussed by Eichler *et al.* [3]. In the corresponding energy range, the photoelectric angular distributions exhibit already a significant forward peaking. This deviation from a simple dipole pattern comes about by contributions of high multipole components in the expansion of the photon wave function in the matrix element (1). As has been pointed out by Spindler *et al.* in 1979 [12], even for nonrelativistic collisions, the effect of the retardation (i.e., higher multipole terms) of the photon wave function and the transformation (2,3) to the laboratory frame balance each other, in such a way that one obtains a $\sin^2\theta$ distribution. Hence, while the importance of higher multipole moments for the inverse reaction to the photoelectric effect has been known for a long time [9,12], the contribution of quadrupole terms to the photoelectric effect itself has been discovered just recently in the case of soft x rays [13].

While in the energy range up to 1.0 GeV/u spin-flip contributions and hence the deviation from a $\sin^2\theta$ distribution play a minor role, the situation changes at 2.0 GeV/u, where the spin-flip contribution exceeds the non-spin-flip contribution in the angular range around 30°. At still higher energies, the spin-flip contribution is completely dominant in the whole range of forward angles. It is interesting to observe that the spin-flip part has a minimum between 90° and 120° but rises again at backward angles. The photoionization cross sections at these high energies are much more peaked forward and become negligible beyond 30°. In fact, in deriving the RR cross sections from the photoelectric cross sections, the ratio of the phase spaces and, in particular, the Lorentz transform expressed by Eqs. (2) and (3), lead to a stretching of the angular distributions to larger angles. It has been suggested by Stöhlker [14] that from the experimental point of view, a measurement of RR differential cross sections may be the most practical way to indirectly determine differential photoionization cross sections at high photon energies.

Figures 3 and 4 are similar to Figs. 1 and 2; however, it is seen that the effects of spin-flip transitions are more pro-

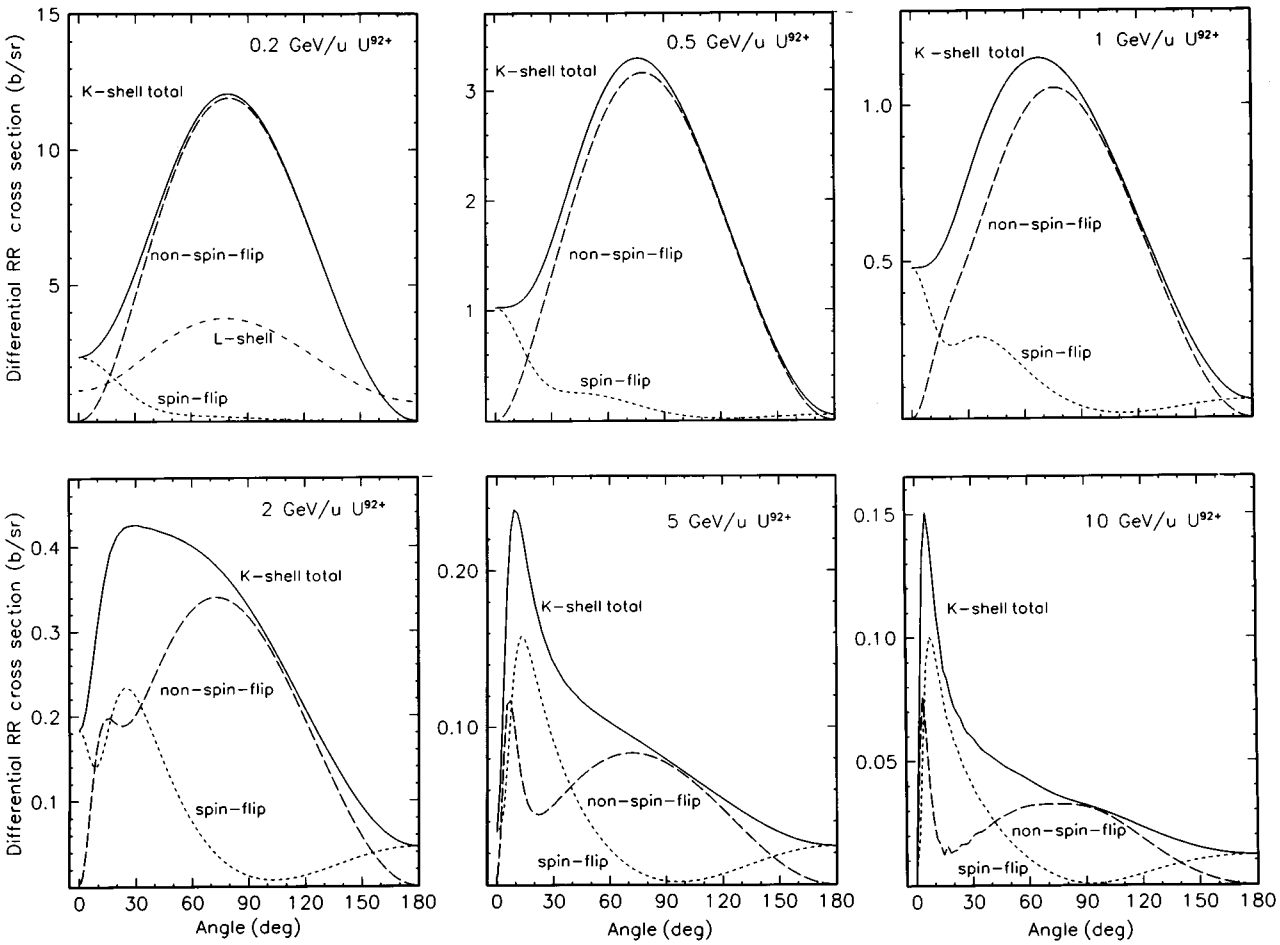

FIG. 3. Exact angle-differential cross sections for radiative recombination of free electrons with the K shell of U^{92+} projectiles with energies from 0.2 to 10.0 GeV/u. The spin-flip and non-spin-flip contributions are shown separately. For the energy of 0.2 GeV/u, the summed cross section for capture into the L shell is also shown.

nounced for the higher projectile charge. In Fig. 3, we have included capture into the L shell only for the lowest energy considered.

Tables I–IV contain the total cross sections corresponding to Figs. 1 to 4. The spin-flip and the non-spin-flip parts are listed separately, as well as the ratio between both. The photon energies E_γ in Tables II and IV are the accurate values associated with the approximate numbers given in Figs. 2 and 4 and with the energies E_P in Tables I and III. The ratios between spin-flip and non-spin-flip total cross sections, which are the same for RR and for photoionization, are seen to increase drastically from 2% at 0.2 GeV/u up to about 50% at 10.0 GeV/u. This again illustrates the important influence of the electron spin in relativistic collisions.

B. Comparison of REC with RR cross sections

Although we have already confirmed earlier [3] that for high-Z projectiles and low-Z targets and collision energies greater than about 100 MeV/u, differential REC and RR cross sections differ only on the percent level, we have reexamined this problem for the AGS energy of 10.8 GeV/u and Au^{79+} projectiles on Au targets [15]. In this case, we have a high-Z target so that for the inner shells the impulse approximation is adequate only because of the very high collision energy with a Lorentz factor $\gamma = 12.6$. This approximation represents the target electrons as free electrons with the momentum distribution (with respect to the target nucleus) calculated from the Fourier transform of the target wave function [1,2]. Since these calculations are very time-consuming, because one has to integrate over the momentum distribution of each target electron, we derive results only for the angle of $\theta = 90°$ and for the s electrons of each shell, see Table V. In all cases, the momentum distribution is calcu-

TABLE I. Cross sections for radiative recombination into the K shell of Au^{79+} for the projectile energy E_P. The cross sections $\sigma_{\text{non-flip}}$ for non-spin-flip transitions and $\sigma_{\text{spin-flip}}$ for spin-flip transitions are shown separately. The last column gives the ratio $\sigma_{\text{spin-flip}}/\sigma_{\text{non-flip}}$. The number in square brackets denotes the power of 10 by which the preceding number has to be multiplied.

E_P (GeV/u)	$\sigma_{\text{non-flip}}$ (b)	$\sigma_{\text{spin-flip}}$ (b)	σ_{total} (b)	Ratio
0.2	6.58 [1]	1.17 [0]	6.70 [1]	0.02
0.5	1.56 [1]	7.47 [−1]	1.64 [1]	0.05
1	4.86 [0]	5.77 [−1]	5.43 [0]	0.12
2	1.53 [0]	3.86 [−1]	1.91 [0]	0.25
5	3.71 [−1]	1.72 [−1]	5.43 [−1]	0.46
10	1.45 [−1]	9.17 [−2]	2.37 [−1]	0.63

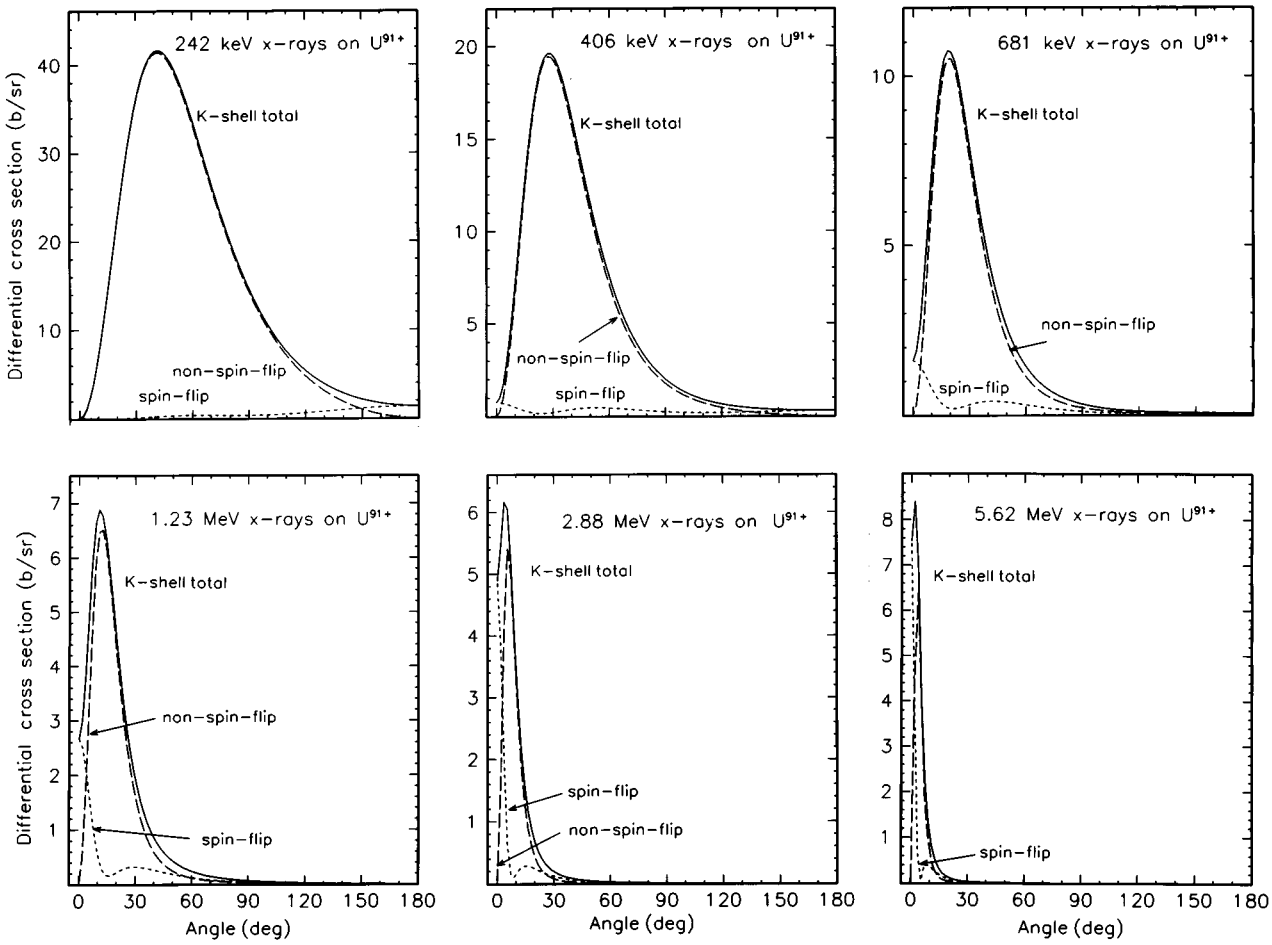

FIG. 4. Exact angle-differential cross sections for photoionization from the K shell of hydrogenlike U^{91+} ions. The x-ray energies given correspond to the projectile energies used in Fig. 3.

lated from nonrelativistic Roothaan-Hartree-Fock wave functions in the double-ζ approximation [11]. For the two innermost shells, we use nonrelativistic Hartree-Fock energies (consistent with the wave functions) or, alternatively, relativistic hydrogenic energies. While for the outer shells, the momentum distribution is very narrow, it becomes increasingly wide for the inner shells. After integrating over the photon line width reflecting the momentum distribution, the differential cross section is no longer sensitive to details. For the L shell, we verify that the contribution from the $2p$ state is similar to that of the $2s$ state. We therefore may assume that in all cases, the shells with higher angular momenta behave as the $l=0$ states. The calculated ratio $\sigma_{\mathrm{REC}}/\sigma_{\mathrm{RR}}$ of the REC cross section to the RR cross section differs very little from 1, in particular for the outer shells which carry the overwhelming weight n^2. Hence inaccuracies in the momentum distribution of the inner target shells and a possible distortion of the continuum electronic wave function will not have much of an effect. After summing over all shells, the binding effects in the target yield a reduction of the REC cross section with respect to RR by only a few percent. We conclude that the total REC cross section for a neutral target may well be represented by the RR cross section for a single electron multiplied by the number of target electrons.

TABLE II. Cross sections for K-shell photoionization of Au^{78+} for the photon energy E_γ. The cross sections represent the sum over the two initial K-shell states. See also caption of Table I.

E_γ (keV)	$\sigma_{\text{non-flip}}$ (b)	$\sigma_{\text{spin-flip}}$ (b)	σ_{total} (b)	Ratio
203.13	1.98 [2]	3.52 [0]	2.02 [2]	0.02
367.70	4.10 [1]	1.97 [0]	4.30 [1]	0.05
642	1.02 [1]	1.21 [0]	1.14 [1]	0.12
1190.6	2.50 [0]	6.32 [−1]	3.14 [0]	0.25
2836.3	4.76 [−1]	2.19 [−1]	6.95 [−1]	0.46
5579.3	1.67 [−1]	1.04 [−1]	2.71 [−1]	0.63

TABLE III. Cross sections for radiative recombination into the K shell of U^{92+}. See caption of Table I.

E_P (GeV/u)	$\sigma_{\text{non-flip}}$ (b)	$\sigma_{\text{spin-flip}}$ (b)	σ_{total} (b)	Ratio
0.2	1.01 [2]	2.93 [0]	1.04 [2]	0.03
0.5	2.68 [1]	1.65 [0]	2.84 [1]	0.06
1	9.01 [0]	1.17 [0]	1.02 [1]	0.13
2	2.98 [0]	7.22 [−1]	3.70 [0]	0.24
5	7.42 [−1]	2.97 [−1]	1.04 [0]	0.40
10	2.91 [−1]	1.46 [−1]	4.36 [−1]	0.50

TABLE IV. Cross sections for K-shell photoionization of U^{91+} for the photon energy E_γ. See the caption of Table II.

E_γ (keV)	$\sigma_{\text{non-flip}}$ (b)	$\sigma_{\text{spin-flip}}$ (b)	σ_{total} (b)	Ratio
241.81	2.14 [2]	6.21 [0]	2.21 [2]	0.03
406.38	5.76 [1]	3.56 [0]	6.12 [1]	0.06
680.67	1.68 [1]	2.17 [0]	1.89 [1]	0.13
1229.3	4.59 [0]	1.11 [0]	5.70 [0]	0.24
2875	9.27 [−1]	3.68 [−1]	1.30 [0]	0.40
5617.9	3.29 [−1]	1.64 [−1]	4.92 [−1]	0.50

IV. CONCLUDING REMARKS

We present a systematics of differential and total cross sections for radiative recombination as an excellent approximation to radiative electron capture into relativistic high-Z projectiles from low-Z target atoms. The calculated differential cross sections have been carried to unprecedented high collision energies. With increasing energy, the cross sections become increasingly peaked in the forward direction and are more and more dominated by spin-flip contributions. The associated cross sections for photoionization are also presented. They are much more peaked towards forward angles (indicating high multipolarities) than the RR cross sections, which are stretched apart by the Lorentz transformation. It is illustrated that at high photon energies, because of this stretching, it is more practical to measure differential cross sections for photoionization in the form of radiative recombination. For a particular example, we show the difference between REC calculations (based on the impulse approximation and Hartree-Fock momentum distributions) and RR calculations for free electrons. The binding in the target leads to a reduction of the cross section on the percent level.

TABLE V. REC differential cross sections for 10.8 GeV/u Au^{79+} ions on Au targets at 90^o laboratory angle. For all occupied ns shells, the binding energy E_b and the REC cross section per target electron is given. The last column gives the ratio to the RR cross section of 0.0163 b/sr. The numbers in square brackets give the power of 10 by which the preceding number has to be multiplied.

Shell	E_b (keV)	σ_{REC} (b/sr)	$\sigma_{\text{REC}}/\sigma_{\text{RR}}$
$1s_{1/2}$	7.37 [1][a]	0.86 [−2]	0.52
$1s_{1/2}$	9.34 [1][b]	0.79 [−2]	0.48
$2s_{1/2}$	1.24 [1][a]	1.46 [−2]	0.90
$2s_{1/2}$	2.39 [1][b]	1.40 [−2]	0.86
$3s_{1/2}$	2.97 [0][a]	1.58 [−2]	0.97
$4s_{1/2}$	6.61 [−1][a]	1.60 [−2]	0.98
$5s_{1/2}$	1.03 [−1][a]	1.61 [−2]	0.99
$6s_{1/2}$	5.86 [−2][a]	1.60 [−2]	0.98

[a]Nonrelativistic Hartree-Fock energy.
[b]Relativistic single-electron energy.

ACKNOWLEDGMENTS

One of the authors (J.E.) gratefully acknowledges the hospitality of Professor N. Toshima and the support of the Japan Society for the Promotion of Science at the University of Tsukuba, where this work was started.

[1] For a summary of relativistic atomic collisions, see, e.g., J. Eichler and W.E. Meyerhof, *Relativistic Atomic Collisions* (Academic Press, San Diego, 1995).
[2] A. Ichihara, T. Shirai, and J. Eichler, Phys. Rev. A **49**, 1975 (1994).
[3] J. Eichler, A. Ichihara, and T. Shirai, Phys. Rev. A **51**, 3027 (1995).
[4] Th. Stöhlker, P.H. Mokler, K. Beckert, F. Bosch, H. Eickhoff, B. Franzke, H. Geissel, M. Jung, T. Kandler, O. Klepper, C. Kozhuharov, R. Moshammer, F. Nickel, F. Nolde, H. Reich, P. Rymuza, C. Scheidenberger, P. Spädtke, Z. Stachura, M. Steck, and A. Warczak, Nucl. Instrum. Methods B **87**, 64 (1994).
[5] Th. Stöhlker, H. Geissel, H. Irnich, T. Kandler, C. Kozhuarov, P.H. Mokler, G. Münzenberg, F. Nickel, C. Scheidenberger, T. Suzuki, M. Kucharski, A. Warczak, P. Rymuza, Z. Stachura, A. Kriessbach, D. Dauvergne, B. Dunford, J. Eichler, A. Ichihara, and T. Shirai, Phys. Rev. Lett. **73**, 3520 (1994).
[6] Th. Stöhlker, C. Kozhuarov, P.H. Mokler, A. Warczak, F. Bosch, H. Geissel, R. Moshammer, C. Scheidenberger, J. Eichler, A. Ichihara, T. Shirai, Z. Stachura, and P. Rymuza, Phys. Rev. A **51**, 2098 (1995).
[7] Th. Stöhlker, F. Bosch, H. Geissel, T. Kandler, C. Kozhuarov, P.H. Mokler, R. Moshammer, P. Rymuza, C. Scheidenberger, Z. Stachura, A. Warczak, J. Eichler, A. Ichihara, and T. Shirai, Nucl. Instrum. Methods Phys. Res. B **98**, 235 (1995).
[8] T. Kandler, Th. Stöhlker, P.H. Mokler, C. Kozhuharov, H. Geissel, C. Scheidenberger, P. Rymuza, Z. Stachura, A. Warczak, R.W. Dunford, J. Eichler, A. Ichihara, and T. Shirai, Z. Phys. D **35**, 35 (1995).
[9] R. Anholt, W.E. Meyerhof, Ch. Stoller, E. Morenzoni, S.A. Adriamonje, J.D. Molitoris, D.H.H. Hoffmann, H. Bowman, J.-S. Xu, Z.-Z. Xu, and J.O. Rasmussen, Phys. Rev. Lett. **53**, 234 (1984).
[10] W.R. Alling and W.R. Johnson, Phys. Rev. **139**, A1050 (1965).
[11] E. Clementi and C. Roetti, At. Data Nucl. Data Tables **14**, 177 (1974).
[12] E. Spindler, H.-D. Betz, and F. Bell, Phys. Rev. Lett. **42**, 832 (1979).
[13] B. Krässig, M. Jung, D.S. Gemmell, E.P. Kanter, T. LeBrun, S.H. Southworth, and L. Young, Phys. Rev. Lett. **75**, 4736 (1995).
[14] Th. Stöhlker (private communication).
[15] H. Gould (private communication).